RESEARCH ARTICLE

Relaxed Static Output Stabilization of Polynomial Fuzzy Control Systems by Lagrange Membership Functions

Zhiyong Bao | **Sike Li** | **Xiaomiao Li** | **Yuehao Du** | **Fucai Liu**

School of Electrical Engineering, Yanshan
University, Qinhuangdao, China

Correspondence
Xiaomiao Li, School of Electrical
Engineering,Yanshan University,Qinhuangdao,
China
Email: xiaomiaoli@ysu.edu.cn

Abstract

This paper is concerned with the stability analysis of the static output-feedback polynomial fuzzy-model-based (SOF PFMB) control systems through designing a novel membership grade integration (MGI) approach. The nonconvex problems of the SOF PFMB control systems are convexificated into the convex conditions by introducing block diagonal positive-definite Lyapunov matrix and nonsingular transformation matrix. We proposed a new approximated membership functions, i.e. Lagrange Membership Functions (LMFs) method, which can be introduced into the stabilization process to relieve the stability conservativeness results. The LMFs are general representations of piecewise-linear membership functions (PLMFs), which makes the number of stability conditions not limited by the number of sample points. In a fixed subdomain, arbitrary sample points can be employed by the LMFs method and achieve higher approximation capability by increasing more sample points, so that membership grades can be incorporated into the system analysis. Furthermore, a novel MGI approach including the information of premise variables and LMFs are proposed, which can make the stability conditions more relaxed. Finally, a simulation example is given to show the merits of the developed techniques.

KEYWORDS
nonlinear control, control design, stability, relaxed stability conditions, polynomial fuzzy system, Lagrange membership functions (LMFs)

1 | INTRODUCTION

As most applications that actually exist are nonlinear, the stability and performance analysis of nonlinear systems received considerable attention of many researchers[1]. Based on the Lyapunov stability theory, a variety types of controllers are proposed, among which the state feedback controller is the most basic and simplest one. However, in practical systems, the full system states are always unmeasurable. Compared with the control method based on full system states, the static output-feedback (SOF) control method only uses the output states, meanwhile, it is simpler than dynamic output-feedback control[2]. Therefore, SOF designs have received more and more attention.

Due to the existence of the output matrix, there will be nonconvex terms in the stability conditions. To circumvent the problem, some achievements based on linear matrix inequalities (LMIs) algorithm have been published, such as, cone complementary linearization[3,4], iterative LMI algorithm[5,6], min/max algorithm[7], transformation algorithm[8], equality constraints[9], etc. Based on these algorithms[10,11,3,4,5,6,7,8,9], many SOF Takagi-Sugeno (T-S) fuzzy system control and synthesis methods[12,13,14,15,16] have been published, for example, in[14], the robust H_{∞} control of T-S fuzzy systems with parameter uncertainty has been investigated; In[15], a novel sufficient condition for the existence of SOF controllers based on parallel distributed compensation (PDC) design was proposed; In[16], a piecewise affine SOF controller was designed for T-S fuzzy system with H_{∞} performance.

In recent years, the polynomial fuzzy system[17] has been proposed, which could expand the range of expressing a nonlinear systems. It is worth noting that for the polynomial fuzzy systems, the sum of squares (SOS)[18] technique must be employed instead of the LMI algorithm to obtain feasible solutions. Until now, there are relatively few research results on polynomial fuzzy systems with SOF controller. In[19,20], a SOF controller was designed to control the positive polynomial fuzzy system.

However, different from the stability analysis of positive polynomial fuzzy systems, the general polynomial fuzzy system stability conditions usually contain the output matrix and Lyapunov matrix, which makes the non-convexity more complicated. In [21], a homogeneous polynomial Lyapunov function was designed to synthesize the SOF controller. Nonetheless, this approach is relatively complex and requires two steps to achieve the control of systems. In [22], a two-step approach was proposed for the first time to remove the long-standing constraint that only the state variables associated with the rows of zeros in the input matrix can be employed to construct the Lyapunov function candidate. Since any state variables can be selected when designing Lyapunov function candidate, the elimination of this constraint will result in more relaxed stability conditions. Furthermore, the imperfect premise matching (IPM) concept was widely employed to achieve a lower computational complexity and higher design flexibility of the controllers [1,23,24,25,26], which makes the controller design not be restricted by the PDC approach, and can freely design the shape and/or the number of fuzzy rules related. However, it cannot apply the properties of some PDC-based analysis approaches, which may lead to relative conservative stability conditions. To deal with this problem caused by the IPM design concept, the membership grade integration (MGI) analysis was designed in [26,24], which can decrease the conservativeness of stability conditions by means of considering the membership grades into the performance/stability analysis [27,28,23,26,24,29,25,30,31,32,33,34,35,36,37,38].

In terms of the MGI analysis method, some types of approximate membership functions have been proposed, for example, polynomial membership functions (PMFs) [30,31], Chebyshev membership functions (CMFs) [32] and so on [33,34,35]. In [30,31], the stability including PMFs are given, nonetheless, the algorithm for determining PMFs is not illustrated. In [32], the CMFs can get the best implementation approach of PMFs through Remez iterative algorithm. However, the systematic way of determining the basis functions of CMFs is not given. In [33], PLMFs was proposed, where the values of sample points are considered, and as the number of sample points increases, the stability results can be more relaxed. Nonetheless, the increased stability conditions will also increase the computational burden. In [34,35], a novel method to approximate original membership functions, i.e., TSMFs method, was proposed, which was obtained by interpolating the Taylor expansion of sample points and was a systematic way of PMFs method. However, it is similar to the PLMFs method that the number of stability conditions is directly related to the number of sample points. On one hand, more sample points will lead to more relaxed stability conditions. On the other hand, more sample points will result in high computational complexity. Therefore, how to obtain the relaxed stability conditions without increasing the number of sample points is a concern, which is worth of further research effort.

Inspired by the above IPM concept and these MGI methods, this paper proposed a novel approximate membership function method to achieve the less conservativeness results. In this paper, more sample points can be chosen in a fixed subdomain to construct the approximate membership functions, which is different to the PLMFs and TSMFs method that only two endpoints in each system state variable are selected as sample points. The formulation of approximate membership functions, i.e., Lagrange membership functions (LMFs), are represented as a weighted sum of membership grades of chosen sample points with corresponding interpolation basis functions based on the Lagrange interpolation theory [39]. According to the LMFs method, PLMFs are only a special case of LMFs when the sample points are two endpoints in each system state variable in a given domain. Meanwhile, LMFs are a systematic way of PMFs, because they are finally introduced in the form of polynomials in stability conditions, and can be used as the specific implementation method of the basic functions in the CMFs method. Thus, without increasing the number of stability conditions, LMFs can use more membership function information to obtain the relaxed stability conditions.

To summarize, the main work in the paper is to design the novel MGI approach for nonlinear systems, and design the feedback gains of the SOF controllers under the IPM concept. The contributions in this paper can be summarized as follows:

1) The nonconvex terms are transformed into convex terms in the stability analysis by choosing block diagonal positive-definite Lyapunov matrix and nonsingular transformation matrix.
2) A novel method of approximate membership functions is proposed. Unlike the existing techniques such as PLMFs and TSMFs, the proposed LMFs method demonstrates a favourable characteristic that the number of sample points can be selected discretionarily without increasing the number of stability conditions. In addition, LMFs are incorporated in the form of polynomials in the stability conditions, which is a systematic way of PMFs method, and can be used as the specific implementation method of the basic functions of CMFs method.
3) Under the proposed novel MGI technique, the obtained stability conditions can include both the regional premise variable information and the membership function information provided by LMFs, which leads to the relaxed stability results.

The remainder of this paper is as follows. The polynomial fuzzy model of nonlinear plants and the corresponding static output-feedback controllers are introduced in Section 2. Section 3 gives the main results, including basic stability conditions,

LMFs algorithm implementation and the novel MGI analysis method combining LMFs and premise variables. Section 4 show the merits of the developed techniques by a nonlinear example. Finally, this paper is concluded in Section 5.

Notations: Throughout this paper, the form of a monomial is a function of $x_1^{z_1}(t), x_2^{z_2}(t), \ldots, x_n^{z_n}(t)$, where z_i, $i = 1, \ldots, n$, is a non-negative integer. A finite number of monomials can be formed to a polynomial $\Upsilon(\mathbf{x}(t))$ by the linear combination. An SOS refers to the polynomial $\Upsilon(\mathbf{x}(t))$ with the property of $\Upsilon(\mathbf{x}(t)) = \sum_{j=1}^{m} \Phi_j(\mathbf{x}(t))^2$, where $\Phi_j(\mathbf{x}(t))$ can be an arbitrary polynomial and m is a positive integer. Furthermore, a positive (negative) definite matrix P means $P > 0$ ($P < 0$).

2 | PRELIMINARIES

2.1 | Polynomial Fuzzy Model with Output

A polynomial fuzzy model for the nonlinear plant composed of p fuzzy rules, where the ith rule:

$$\text{Rule } i : \text{IF } f_1(\mathbf{x}(t)) \text{ is } M_1^i \text{ AND} \cdots \text{AND } f_\psi(\mathbf{x}(t)) \text{ is } M_\psi^i$$
$$\text{THEN } \dot{\mathbf{x}}(t) = \mathbf{A}_i(\mathbf{x}(t))\hat{\mathbf{x}}(\mathbf{x}(t)) + \mathbf{B}_i(\mathbf{x}(t))\mathbf{u}(t),$$
$$\mathbf{y}(t) = \mathbf{C}\hat{\mathbf{x}}(\mathbf{x}(t)), i = 1, ..., p, \tag{1}$$

where $\hat{\mathbf{x}}(\mathbf{x}(t)) \in \Re^N$ is a monomial vector that is arbitrary independent of the system states $\mathbf{x}(t)$; $\mathbf{A}_i(\mathbf{x}(t)) \in \Re^{n \times N}$, $\mathbf{B}_i(\mathbf{x}(t)) \in \Re^{n \times m}$ are the given polynomial matrices; $\mathbf{C} \in \Re^{d \times N}$ is the constant matrix; $\mathbf{y}(t) \in \Re^d$ is the vector.

According to the above description of fuzzy rules, the whole system dynamics are described as:

$$\dot{\mathbf{x}}(t) = \sum_{i=1}^{p} \omega_i(\mathbf{x}(t))(\mathbf{A}_i(\mathbf{x}(t))\hat{\mathbf{x}}(\mathbf{x}(t)) + \mathbf{B}_i(\mathbf{x}(t))\mathbf{u}(t)),$$
$$\mathbf{y}(t) = \mathbf{C}\hat{\mathbf{x}}(\mathbf{x}(t)), \tag{2}$$

where $\sum_{i=1}^{p} \omega_i(\mathbf{x}(t)) = 1$; $\omega_i(\mathbf{x}(t)) = \dfrac{\prod_{\alpha=1}^{\psi} \mu_{M_\alpha^i}(f_\alpha(\mathbf{x}(t)))}{\sum_{k=1}^{p} \prod_{\alpha=1}^{\psi} \mu_{M_\alpha^k}(f_\alpha(\mathbf{x}(t)))} \geq 0$, where $\mu_{M_\alpha^i}(f_\alpha(\mathbf{x}(t)))$ is the grade of membership corresponding to the fuzzy set of M_α^i.

2.2 | Static Output-Feedback (SOF) Polynomial Fuzzy Controller

With the IPM concept, let c be the number of fuzzy rules describing the controller, and the jth rule is of the following format:

$$\text{Rule } j : \text{IF } g_1(\mathbf{y}(t)) \text{ is } N_1^j \text{ AND} \cdots \text{AND } g_\Omega(\mathbf{y}(t)) \text{ is } N_\Omega^j$$
$$\text{THEN } \mathbf{u}(t) = \mathbf{G}_j(\mathbf{y}(t))\mathbf{y}(t), j = 1, ..., c, \tag{3}$$

where $\mathbf{G}_j(\mathbf{y}(t)) \in \Re^{m \times d}$, $j = 1, ..., c$, are the polynomial feedback gains to be obtained; N_β^j is the fuzzy set of rule j corresponding to the premise variable $g_\beta(\mathbf{x}(t))$, with $\beta = 1, ..., \Omega$.

The dynamics of SOF polynomial fuzzy controller are:

$$\mathbf{u}(t) = \sum_{j=1}^{c} m_j(\mathbf{y}(t))\mathbf{G}_j(\mathbf{y}(t))\mathbf{y}(t), \tag{4}$$

where $\sum_{j=1}^{c} m_j(\mathbf{y}(t)) = 1$; $m_j(\mathbf{y}(t)) = \dfrac{\prod_{\beta=1}^{\Omega} \mu_{N_\beta^j}(g_\beta(\mathbf{y}(t)))}{\sum_{k=1}^{c} \prod_{\beta=1}^{\Omega} \mu_{N_\beta^k}(g_\beta(\mathbf{y}(t)))} \geq 0$; $u_{N_\beta^j}(g_\beta(\mathbf{y}(t)))$ is the grade of membership corresponding to the fuzzy set N_β^j.

Due to $\mathbf{y}(t) = \mathbf{C}\hat{\mathbf{x}}(\mathbf{x}(t))$, we have

$$\mathbf{u}(t) = \sum_{j=1}^{c} m_j(\mathbf{y}(t))\mathbf{G}_j(\mathbf{y}(t))\mathbf{C}\hat{\mathbf{x}}(\mathbf{x}(t)). \tag{5}$$

According to (2) and (5), the SOF PFMB control system is obtained as:

$$\dot{\mathbf{x}}(t) = \sum_{i=1}^{p}\sum_{j=1}^{c}\omega_i(\mathbf{x}(t))m_j(\mathbf{y}(t))\left(\mathbf{A}_i(\mathbf{x}(t)) + \mathbf{B}_i(\mathbf{x}(t))\mathbf{G}_j(\mathbf{y}(t))\mathbf{C}\right)\hat{\mathbf{x}}(\mathbf{x}(t)). \tag{6}$$

Remark 1. The IPM concept [1,24,36] means that the control engineers can freely design the shape of the membership functions and/or the number of fuzzy rules of the polynomial fuzzy controller. However, it should be noted that the increased design flexibility of the controller also brings about the problem of conservative stability conditions.

Through the above description, the system can be established, as the structure diagram of polynomial fuzzy system control scheme is shown in Figure 1 .
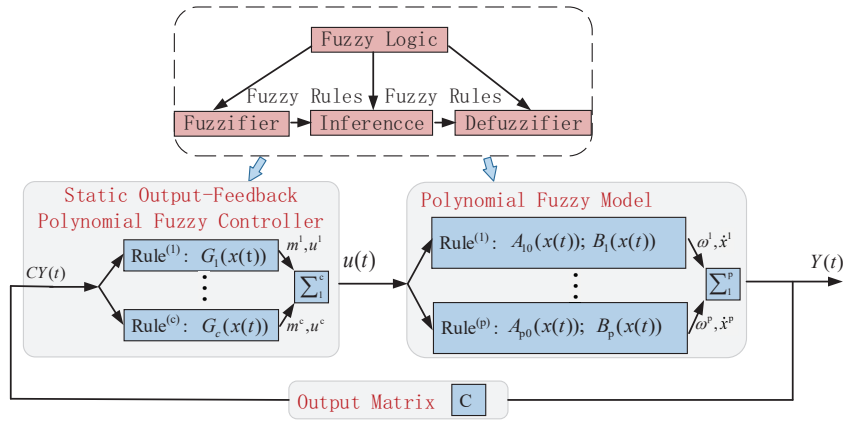

FIGURE 1 Structure diagram of SOF PFMB system control scheme.

3 | STABILITY ANALYSIS

3.1 | Stability Analysis of SOF PFMB Control System

In the following of this paper, for brevity, $\mathbf{x}(t)$, $\mathbf{y}(t)$, $\hat{\mathbf{x}}(\mathbf{x}(t))$, $\omega_i(\mathbf{x}(t))$ and $m_j(\mathbf{y}(t))$ are denoted as $\mathbf{x}$, $\mathbf{y}$, $\hat{\mathbf{x}}$, $\omega_i(\mathbf{x})$ and $m_j(\mathbf{y})$, respectively. From (6), we obtain

$$\begin{aligned}\dot{\hat{\mathbf{x}}} &= \frac{\partial\hat{\mathbf{x}}}{\partial\mathbf{x}}\frac{d\mathbf{x}}{dt} = \mathbf{T}(\mathbf{x})\dot{\mathbf{x}}\\ &= \sum_{i=1}^{p}\sum_{j=1}^{c}\omega_i(\mathbf{x})m_j(\mathbf{y})(\mathbf{T}(\mathbf{x})\mathbf{A}_i(\mathbf{x}) + \mathbf{T}(\mathbf{x})\mathbf{B}_i(\mathbf{x})\mathbf{G}_j(\mathbf{y})\mathbf{C})\hat{\mathbf{x}},\end{aligned} \tag{7}$$

where the $(i,j)^{th}$ element of the polynomial matrix $\mathbf{T}(\mathbf{x})$ has $T_{ij}(\mathbf{x}) = \partial\hat{x}_i(\mathbf{x})/\partial x_j$.

The nonconvex stability conditions may be caused by the polynomial feedback gain and the Lyapunov function matrix. To circumvent this problem, a constant transformation matrix $\mathbf{\Gamma} \in \Re^{N \times N}$ [8] is introduced as follows:

Lemma 1. *Define*

$$\mathbf{\Gamma} = [\mathbf{C}^T(\mathbf{CC}^T)^{-1} \, ortc(\mathbf{C}^T)] \in \Re^{N \times N}, \tag{8}$$

where $ortc(\mathbf{C}^T)$ is the orthogonal complement of $\mathbf{C}^T$. Thus, for identity matrix $\mathbf{I}_d \in \Re^{d \times d}$, we can get

$$\mathbf{C\Gamma} = [\mathbf{I}_d \; \mathbf{0}] \in \Re^{d \times N}, \tag{9}$$

Assuming that $\mathbf{\Gamma}^{-1}$ exists, we transform the state vector $\hat{\mathbf{x}}$ according to $\hat{\mathbf{z}} = \mathbf{\Gamma}^{-1}\hat{\mathbf{x}}$, then

$$\begin{aligned}
\dot{\hat{\mathbf{z}}} &= \mathbf{\Gamma}^{-1}\dot{\hat{\mathbf{x}}} \\
&= \sum_{i=1}^{p}\sum_{j=1}^{c} \omega_i(\mathbf{x})m_j(\mathbf{y})(\tilde{\mathbf{A}}_i(\mathbf{x})\mathbf{\Gamma} + \tilde{\mathbf{B}}_i(\mathbf{x})\mathbf{G}_j(\mathbf{y})\mathbf{C\Gamma})\hat{\mathbf{z}},
\end{aligned} \tag{10}$$

where $\mathbf{\Gamma}$ is as defined in Lemma 1, $\tilde{\mathbf{A}}_i(\mathbf{x}) = \mathbf{\Gamma}^{-1}\mathbf{T}(\mathbf{x})\mathbf{A}_i(\mathbf{x})$, and $\tilde{\mathbf{B}}_i(\mathbf{x}) = \mathbf{\Gamma}^{-1}\mathbf{T}(\mathbf{x})\mathbf{B}_i(\mathbf{x})$.

Remark 2. Since $\mathbf{\Gamma}$ is a non-singular matrix, the stability of the transformed SOF PFMB system (10) and the SOF PFMB system (6) is consistent.

A Lyapunov function is given to study the stability of the system (10), and its format is

$$V(\mathbf{x}) = \hat{\mathbf{z}}^T \mathbf{P}(\tilde{\mathbf{x}})^{-1}\hat{\mathbf{z}}, \tag{11}$$

where $\tilde{\mathbf{x}} = (x_{k_1}, ..., x_{k_m})$ is the vector to be selected, so that $\mathbf{K} = \{k_1, ..., k_m\}$ represents the indices of the zero rows corresponding to all i in $\mathbf{B}_i(\mathbf{x})$. Inspired by [40], we choose $0 < \mathbf{P}(\tilde{\mathbf{x}}) = \mathbf{P}(\tilde{\mathbf{x}})^T \in \Re^{N \times N}$, which is given as a block diagonal positive-definite polynomial matrix and satisfies

$$\mathbf{P}(\tilde{\mathbf{x}}) = \begin{bmatrix} \mathbf{P}(\tilde{\mathbf{x}})_{11} & \mathbf{0} \\ \mathbf{0} & \mathbf{P}(\tilde{\mathbf{x}})_{22} \end{bmatrix}, \tag{12}$$

where $\mathbf{P}(\tilde{\mathbf{x}})_{11} \in \Re^{d \times d}$ and $\mathbf{P}(\tilde{\mathbf{x}})_{22} \in \Re^{(N-d) \times (N-d)}$.

Derivation of $V(\mathbf{x})$ is given as:

$$\begin{aligned}
\dot{V}(\mathbf{x}) &= \dot{\hat{\mathbf{z}}}^T\mathbf{P}(\tilde{\mathbf{x}})^{-1}\hat{\mathbf{z}} + \hat{\mathbf{z}}^T\mathbf{P}(\tilde{\mathbf{x}})^{-1}\dot{\hat{\mathbf{z}}} + \hat{\mathbf{z}}^T\dot{\mathbf{P}}(\tilde{\mathbf{x}})^{-1}\hat{\mathbf{z}} \\
&= \sum_{i=1}^{p}\sum_{j=1}^{c} \omega_i(\mathbf{x})m_j(\mathbf{y})\hat{\mathbf{z}}^T((\tilde{\mathbf{A}}_i(\mathbf{x})\mathbf{\Gamma} + \tilde{\mathbf{B}}_i(\mathbf{x})\mathbf{G}_j(\mathbf{y})\mathbf{C\Gamma})^T\mathbf{P}(\tilde{\mathbf{x}})^{-1} + \mathbf{P}(\tilde{\mathbf{x}})^{-1}(\tilde{\mathbf{A}}_i(\mathbf{x})\mathbf{\Gamma} + \tilde{\mathbf{B}}_i(\mathbf{x})\mathbf{G}_j(\mathbf{y})\mathbf{C\Gamma}))\hat{\mathbf{z}} + \hat{\mathbf{z}}^T\frac{d\mathbf{P}(\tilde{\mathbf{x}})^{-1}}{dt}\hat{\mathbf{z}}.
\end{aligned} \tag{13}$$

Due to the output vector $\mathbf{y} = \mathbf{C}\hat{\mathbf{x}}$ is related to the system states $\mathbf{x}$, $\mathbf{G}_j(\mathbf{y})$ is actually the function of $\mathbf{x}$. Then, the polynomial feedback gains of the controller are

$$\mathbf{G}_j(\mathbf{y}) = \mathbf{N}_j(\mathbf{x})\mathbf{P}(\tilde{\mathbf{x}})_{11}^{-1}, \tag{14}$$

where $\mathbf{N}_j(\mathbf{x}) \in \Re^{m \times d}, j = 1, ..., c$, can be selected as arbitrary polynomial matrices.

Referring to (13), with (9), (12) and (14), we obtain

$$\begin{aligned}
\tilde{\mathbf{B}}_i(\mathbf{x})\mathbf{G}_j(\mathbf{y})\mathbf{C\Gamma} &= \tilde{\mathbf{B}}_i(\mathbf{x})\mathbf{G}_j(\mathbf{y})[\mathbf{I}_d \quad \mathbf{0}]\mathbf{P}(\tilde{\mathbf{x}})\mathbf{P}(\tilde{\mathbf{x}})^{-1} \\
&= \tilde{\mathbf{B}}_i(\mathbf{x})\mathbf{N}_j(\mathbf{x})\mathbf{P}(\tilde{\mathbf{x}})_{11}^{-1}[\mathbf{I}_d \quad \mathbf{0}]\mathbf{P}(\tilde{\mathbf{x}})\mathbf{P}(\tilde{\mathbf{x}})^{-1} \\
&= \tilde{\mathbf{B}}_i(\mathbf{x})[\mathbf{N}_j(\mathbf{x}) \quad \mathbf{0}]\mathbf{P}(\tilde{\mathbf{x}})^{-1}.
\end{aligned} \tag{15}$$

To handle the term $\frac{d\mathbf{P}(\tilde{\mathbf{x}})^{-1}}{dt}$ in (13), we quote the results in [17], thus,

$$\frac{d\mathbf{P}(\tilde{\mathbf{x}})^{-1}}{dt} = \sum_{k \in \mathbf{K}} \frac{\partial \mathbf{P}(\tilde{\mathbf{x}})^{-1}}{\partial x_k} \frac{dx_k}{dt}$$

$$= \sum_{k \in \mathbf{K}} -\mathbf{P}(\tilde{\mathbf{x}})^{-1} \frac{\partial \mathbf{P}(\tilde{\mathbf{x}})}{\partial x_k} \mathbf{P}(\tilde{\mathbf{x}})^{-1} \sum_{i=1}^{p} \sum_{j=1}^{c} \omega_i(\mathbf{x}) m_j(\mathbf{y}) \left(\mathbf{A}_i^k(\mathbf{x}) + \mathbf{B}_i^k(\mathbf{x}) \mathbf{G}_j(\mathbf{y}) \mathbf{C} \right) \hat{\mathbf{x}}. \tag{16}$$

By choosing a specific vector $\tilde{\mathbf{x}}$, we can get rid of the nonconvex term $\mathbf{B}_i^k(\mathbf{x}) \mathbf{G}_j(\mathbf{y}) \mathbf{C}$ in the stability conditions. Hence

$$\frac{d\mathbf{P}(\tilde{\mathbf{x}})^{-1}}{dt} = \sum_{k \in \mathbf{K}} -\mathbf{P}(\tilde{\mathbf{x}})^{-1} \frac{\partial \mathbf{P}(\tilde{\mathbf{x}})}{\partial x_k} \mathbf{P}(\tilde{\mathbf{x}})^{-1} \sum_{i=1}^{p} \omega_i(\mathbf{x}) \mathbf{A}_i^k(\mathbf{x}) \hat{\mathbf{x}}. \tag{17}$$

Defining $\mathbf{z} = \mathbf{P}(\tilde{\mathbf{x}})^{-1} \hat{\mathbf{z}}$, and from (13), (15) and (17), we can obtain

$$\dot{V}(\mathbf{x}) = \sum_{i=1}^{p} \sum_{j=1}^{c} \omega_i(\mathbf{x}) m_j(\mathbf{y}) \mathbf{z}^T \mathbf{Q}_{ij}(\mathbf{x}) \mathbf{z}, \tag{18}$$

where $\mathbf{Q}_{ij}(\mathbf{x}) = \tilde{\mathbf{A}}_i(\mathbf{x}) \boldsymbol{\Gamma} \mathbf{P}(\tilde{\mathbf{x}}) + \mathbf{P}(\tilde{\mathbf{x}}) \boldsymbol{\Gamma}^T \tilde{\mathbf{A}}_i(\mathbf{x})^T + \tilde{\mathbf{B}}_i(\mathbf{x}) \begin{bmatrix} \mathbf{N}_j(\mathbf{x}) & \mathbf{0} \end{bmatrix} + \begin{bmatrix} \mathbf{N}_j(\mathbf{x}) & \mathbf{0} \end{bmatrix}^T \tilde{\mathbf{B}}_i(\mathbf{x})^T - \sum_{k \in \mathbf{K}} \frac{\partial \mathbf{P}(\tilde{\mathbf{x}})^{-1}}{\partial x_k} \mathbf{A}_i^k(\mathbf{x}) \hat{\mathbf{x}}$, with $i = 1, ..., p; j = 1, ..., c$. Based on the aforementioned stability analysis results, we can draw the following theorem.

Theorem 1. *A SOF PFMB control system* (6) *is asymptotically stable if there exist a block diagonal positive-definite polynomial matrix* $\mathbf{P}(\tilde{\mathbf{x}}) = \mathbf{P}(\tilde{\mathbf{x}})^T = \begin{bmatrix} \mathbf{P}(\tilde{\mathbf{x}})_{11} & \mathbf{0} \\ \mathbf{0} & \mathbf{P}(\tilde{\mathbf{x}})_{22} \end{bmatrix} \in \Re^{N \times N}$ *and polynomial matrices* $\mathbf{N}_j(\mathbf{x}) \in \Re^{m \times d}$, $j = 1, ..., c$, *such that the following conditions hold:*

$$\varsigma^T (\mathbf{P}(\tilde{\mathbf{x}}) - \iota_1(\tilde{\mathbf{x}}) \mathbf{I}) \varsigma \ \text{is SOS}, \tag{19}$$

$$-\varsigma^T (\mathbf{Q}_{ij}(\mathbf{x}) + \iota_2(\mathbf{x}) \mathbf{I}) \varsigma \ \text{is SOS} \ \forall i, j, \tag{20}$$

where $\varsigma \in \Re^N$ *is an arbitrary monomial vector in system states* $\mathbf{x}$; $\iota_1(\tilde{\mathbf{x}}) > 0$ *and* $\iota_2(\mathbf{x}) > 0$ *are given scalar polynomials;* $\mathbf{Q}_{ij}(\mathbf{x}) = \tilde{\mathbf{A}}_i(\mathbf{x}) \boldsymbol{\Gamma} \mathbf{P}(\tilde{\mathbf{x}}) + \mathbf{P}(\tilde{\mathbf{x}}) \boldsymbol{\Gamma}^T \tilde{\mathbf{A}}_i(\mathbf{x})^T + \tilde{\mathbf{B}}_i(\mathbf{x}) \begin{bmatrix} \mathbf{N}_j(\mathbf{x}) & \mathbf{0} \end{bmatrix} + \begin{bmatrix} \mathbf{N}_j(\mathbf{x}) & \mathbf{0} \end{bmatrix}^T \tilde{\mathbf{B}}_i(\mathbf{x})^T - \sum_{k \in \mathbf{K}} \frac{\partial \mathbf{P}(\tilde{\mathbf{x}})^{-1}}{\partial x_k} \mathbf{A}_i^k(\mathbf{x}) \hat{\mathbf{x}}$ *for* $i = 1, ..., p$, $j = 1, ..., c$; *and* $\mathbf{G}_j(\mathbf{y}) = \mathbf{N}_j(\mathbf{x}) \mathbf{P}(\tilde{\mathbf{x}})_{11}^{-1}$.

Remark 3. Theorem 1 is valid for solving controllers with arbitrary shapes of membership functions. However, the absence of membership function will make finding feasible solutions very conservative.

3.2 | Stability Conditions of SOF PFMB Control Systems with MGI approach

To alleviate this problem, the global domain Θ is separated into L subdomains Θ_l, thus, $\Theta = \cup_{l=1}^{L} \Theta_l$, $l = 1, \ldots, L$. Consequently, the nonlinearity of membership functions in a subdomain is less stronger as in the whole domain, which implies relatively lower-order polynomial can be used instead. Specifically, each system state x_r, $r = 1, \cdots, n$, is separated into s_r subdomains, then, $L = \prod_{r=1}^{n} s_r$. Therefore, one has:

$$h_{ij}(\mathbf{x}) = \sum_{l=1}^{L} \sigma_l(\mathbf{x}) (\hat{h}_{ijl}(\mathbf{x}) + \Delta h_{ijl}(\mathbf{x})), \tag{21}$$

where the $\sigma_l(\mathbf{x})$ is a indication function, which satisfies $\sigma_l(\mathbf{x}) = \begin{cases} 1, & \mathbf{x} \in \Theta_l, l = 1, ..., L \\ 0, & otherwise; \end{cases}$ $\Delta h_{ijl}(\mathbf{x})$ is defined as the approximation error of membership functions in each subdomain Θ_l; $\hat{h}_{ijl}(\mathbf{x})$ is a polynomial approximate membership function in each subdomain Θ_l,

From (21), we define $\overline{\gamma}_{ijl}$ as the upper bound of absolute value of approximation error, which satisfies $\left| \Delta h_{ijl}(\mathbf{x}) \right| \leq \overline{\gamma}_{ijl}$. In addition, we introduce some slack matrices $\mathbf{Y}_{ijl}(\mathbf{x})$, which satisfies $\mathbf{Y}_{ijl}(\mathbf{x}) = \mathbf{Y}_{ijl}(\mathbf{x})^T \geq 0$ and $\mathbf{Y}_{ijl}(\mathbf{x}) \geq \mathbf{Q}_{ij}(\mathbf{x})$ to facilitate the

integration of the approximation error $\left| \Delta h_{ijl}(\mathbf{x}) \right|$ into the stability conditions. We get from (18) and (21) that

$$
\begin{aligned}
\dot{V}(\mathbf{x}) &= \sum_{i=1}^{p} \sum_{j=1}^{c} h_{ij}(\mathbf{x}) \mathbf{z}^T \mathbf{Q}_{ij}(\mathbf{x}) \mathbf{z} \\
&= \sum_{l=1}^{L} \sigma_l(\mathbf{x}) \sum_{i=1}^{p} \sum_{j=1}^{c} \mathbf{z}^T \left(\hat{h}_{ijl}(\mathbf{x}) + \Delta h_{ijl}(\mathbf{x}) \right) \mathbf{Q}_{ij}(\mathbf{x}) \mathbf{z} \\
&\leq \sum_{l=1}^{L} \sigma_l(\mathbf{x}) \sum_{i=1}^{p} \sum_{j=1}^{c} \mathbf{z}^T \left(\hat{h}_{ijl}(\mathbf{x}) \mathbf{Q}_{ij}(\mathbf{x}) + \left| \Delta h_{ijl}(\mathbf{x}) \right| \mathbf{Y}_{ijl} \right) \mathbf{z} \\
&\leq \sum_{l=1}^{L} \sigma_l(\mathbf{x}) \sum_{i=1}^{p} \sum_{j=1}^{c} \mathbf{z}^T \left(\sum_{i_1=1}^{\lambda_1} \cdots \sum_{i_n=1}^{\lambda_n} \prod_{r=1}^{n} v_{r i_r l}(x_r) \overline{h}_{iji_1 \cdots i_n l} \mathbf{Q}_{ij}(\mathbf{x}) + \overline{\gamma}_{ijl} \mathbf{Y}_{ijl}(\mathbf{x}) \right) \mathbf{z},
\end{aligned}
\tag{22}
$$

where $v_{r i_r l}(x_r)$ are the Lagrange basis functions for variable x_r, and defined as (31), $\overline{h}_{iji_1 \cdots i_n l}$ are the grades of sample points of $h_{ij}(\mathbf{x})$.

The regional information of premise variables is employed through S-procedure to further relax the stability analysis results. In each subdomain Θ_l, each system state satisfies $x_k \in [x_{k1l}, x_{k2l}]$, $k = 1, ..., n$, $l = 1, ..., L$, where x_{k1l} and x_{k2l} are the boundary values of the system state x_k in Θ_l. Moreover, considering $0 \leq \mathbf{M}_l(\mathbf{x}) = \mathbf{M}_l(\mathbf{x})^T \in \Re^{N \times N}$, $l = 1, ..., L$, the following inequality is obtained as

$$
\sum_{l=1}^{L} \sigma_l(\mathbf{x}) \sum_{k=1}^{n} (x_k - x_{k1l})(x_{k2l} - x_k) \mathbf{M}_l(\mathbf{x}) \geq 0.
\tag{23}
$$

where the indication function $\sigma_l(\mathbf{x})$ has $\sigma_l(\mathbf{x}) = \begin{cases} 1, & \mathbf{x} \in \Theta_l, l = 1, ..., L; \\ 0, & otherwise. \end{cases}$

Furthermore, it can be derived from (22) and (23) that

$$
\begin{aligned}
\dot{V}(\mathbf{x}) &\leq \sum_{l=1}^{L} \sigma_l(\mathbf{x}) \sum_{i=1}^{p} \sum_{j=1}^{c} \mathbf{z}^T \left(\sum_{i_1=1}^{\lambda_1} \cdots \sum_{i_n=1}^{\lambda_n} \prod_{r=1}^{n} v_{r i_r l}(x_r) \overline{h}_{iji_1 \cdots i_n l} \mathbf{Q}_{ij}(\mathbf{x}) + \overline{\gamma}_{ijl} \mathbf{Y}_{ijl}(\mathbf{x}) \right) \mathbf{z} \\
&\leq \sum_{l=1}^{L} \sigma_l(\mathbf{x}) \mathbf{z}^T \left(\sum_{i=1}^{p} \sum_{j=1}^{c} \left(\sum_{i_1=1}^{\lambda_1} \cdots \sum_{i_n=1}^{\lambda_n} \prod_{r=1}^{n} v_{r i_r l}(x_r) \overline{h}_{iji_1 \cdots i_n l} \mathbf{Q}_{ij}(\mathbf{x}) + \overline{\gamma}_{ijl} \mathbf{Y}_{ijl}(\mathbf{x}) \right) + \sum_{k=1}^{n} (x_k - x_{k1l})(x_{k2l} - x_k) \mathbf{M}_l(\mathbf{x}) \right) \mathbf{z}.
\end{aligned}
\tag{24}
$$

Next, a theorem can be derived from the above analysis results.

Theorem 2. *A SOF PFMB control system* (6) *is asymptotically stable if there exist a block diagonal positive-definite polynomial matrix* $\mathbf{P}(\tilde{\mathbf{x}}) = \mathbf{P}(\tilde{\mathbf{x}})^T = \begin{bmatrix} \mathbf{P}(\tilde{\mathbf{x}})_{11} & \mathbf{0} \\ \mathbf{0} & \mathbf{P}(\tilde{\mathbf{x}})_{22} \end{bmatrix} \in \Re^{N \times N}$, $\mathbf{Y}_{ijl}(\mathbf{x}) = \mathbf{Y}_{ijl}(\mathbf{x})^T \in \Re^{N \times N}$, $\mathbf{M}_l(\mathbf{x}) = \mathbf{M}_l(\mathbf{x})^T \in \Re^{N \times N}$, *for all* $i = 1, ..., p$, $j = 1, ..., c$, $l = 1, ..., L$, *such that:*

$$
\varsigma^T (\mathbf{P}(\tilde{\mathbf{x}}) - \iota_1(\tilde{\mathbf{x}}) \mathbf{I}) \varsigma \text{ is SOS,}
\tag{25}
$$

$$
\varsigma^T (\mathbf{M}_l(\mathbf{x}) - \iota_2(\mathbf{x}) \mathbf{I}) \varsigma \text{ is SOS } \forall l,
\tag{26}
$$

$$
\varsigma^T (\mathbf{Y}_{ijl}(\mathbf{x}) - \iota_3(\mathbf{x}) \mathbf{I}) \varsigma \text{ is SOS } \forall i, j, l,
\tag{27}
$$

$$
\varsigma^T (\mathbf{Y}_{ijl}(\mathbf{x}) - \mathbf{Q}_{ij}(\mathbf{x}) - \iota_4(\mathbf{x}) \mathbf{I}) \varsigma \text{ is SOS } \forall i, j, l,
\tag{28}
$$

$$
-\varsigma^T \left(\sum_{i=1}^{p} \sum_{j=1}^{c} \left(\sum_{i_1=1}^{\lambda_1} \cdots \sum_{i_n=1}^{\lambda_n} \prod_{r=1}^{n} v_{r i_r l}(x_r) \overline{h}_{iji_1 \cdots i_n l} \mathbf{Q}_{ij}(\mathbf{x}) + \overline{\gamma}_{ijl} \mathbf{Y}_{ijl}(\mathbf{x}) \right) + \sum_{k=1}^{n} (x_k - x_{k1l})(x_{k2l} - x_k) \mathbf{M}_l(\mathbf{x}) + \iota_5(\mathbf{x}) \mathbf{I} \right) \varsigma \text{ is SOS } \forall l, \tag{29}
$$

where $\varsigma \in \Re^N$ *is an arbitrary monomial vector in system states* $\mathbf{x}$; $\iota_1(\tilde{\mathbf{x}}) > 0$, $\iota_2(\mathbf{x}) > 0$, $\iota_3(\mathbf{x}) > 0$, $\iota_4(\mathbf{x}) > 0$ *and* $\iota_5(\mathbf{x}) > 0$ *are given scalar polynomials;* $\mathbf{Q}_{ij}(\mathbf{x}) = \tilde{\mathbf{A}}_i(\mathbf{x})\mathbf{\Gamma}\mathbf{P}(\tilde{\mathbf{x}}) + \mathbf{P}(\tilde{\mathbf{x}})\mathbf{\Gamma}^T\tilde{\mathbf{A}}_i(\mathbf{x})^T + \tilde{\mathbf{B}}_i(\mathbf{x})\begin{bmatrix} \mathbf{N}_j(\mathbf{x}) & \mathbf{0} \end{bmatrix} + \begin{bmatrix} \mathbf{N}_j(\mathbf{x}) & \mathbf{0} \end{bmatrix}^T \tilde{\mathbf{B}}_i(\mathbf{x})^T - \sum_{k \in \mathbf{K}} \frac{\partial \mathbf{P}(\tilde{\mathbf{x}})^{-1}}{\partial x_k}\mathbf{A}_i^k(\mathbf{x})\hat{\mathbf{x}}$, *for* $i = 1, ..., p$; $j = 1, ..., c$; *and the feedback gains of the controllers can be obtained as* $\mathbf{G}_j(\mathbf{y}) = \mathbf{N}_j(\mathbf{x})\mathbf{P}(\tilde{\mathbf{x}})_{11}^{-1}$.

Remark 4. The number of stability conditions in Theorem 2 is $2pcL+2L+1$, which is directly related to the number of subdomains L. However, the division of domains is positively correlated with computational power consumption. One advantage of LMFs is that when the partition is fixed, using LMFs to represent membership function information can obtain better approximation capacity by using more sample points. When the whole domain is not partitioned, the number of stability conditions will be minimized, which is $2pc + 3$.

Remark 5. According to Remark 8, the LMFs are the extension of PLMFs. When the sample points are two endpoints in each partition, the stability conditions of LMFs and PLMFs are the same. However, LMFs can use more sample points in each partition, thus, more membership function information can be employed to obtain the relaxed stability conditions.

3.3 | Lagrange Membership Functions

The LMFs are proposed in this section, which can be incorporated into the stability conditions of the proposed Theorem 1 to relax the stability analysis results. The output vector $\mathbf{y} = \mathbf{C}\hat{\mathbf{x}}$ is related to the system states $\mathbf{x}$, therefore, $m_j(\mathbf{y})$ is actually a function of $\mathbf{x}$. Moreover, we denote $h_{ij}(\mathbf{x}) = \omega_i(\mathbf{x})m_j(\mathbf{y})$ as the original membership functions.

We define a known bounded n-dimensional operating domain Θ, and make the system states $\mathbf{x} \in \Theta$, $\mathbf{x} = [x_1, \cdots, x_n]^T$. In order to improve the approximation capability of LMFs, higher-order polynomial functions are required, which will also require high computational power to find the feasible solutions.

which can be achieved by LMFs method. The LMFs in each subdomain are defined as

$$\hat{h}_{ijl}(\mathbf{x}) = \sum_{i_1=1}^{\lambda_1} \cdots \sum_{i_n=1}^{\lambda_n} \prod_{r=1}^{n} v_{ri_rl}(x_r)\overline{h}_{iji_1 \cdots i_nl}, \tag{30}$$

where $\overline{h}_{iji_1 \cdots i_nl} \in [0, 1]$ is a constant value of membership functions $h_{ij}(\mathbf{x})$ at the sample points of $\mathbf{x}$ in each subdomain Θ_l; $v_{ri_rl}(x_r)$ is the Lagrange basis function and defined as

$$
\begin{aligned}
v_{ri_rl}(x_r) &= \prod_{i_\beta=1, i_\beta \neq i_r}^{\lambda_r} \frac{x_r - \overline{x}_{ri_\beta l}}{\overline{x}_{ri_rl} - \overline{x}_{ri_\beta l}} \\
&= \frac{(x_r - \overline{x}_{r1l})}{(\overline{x}_{ri_rl} - \overline{x}_{r1l})} \cdots \frac{(x_r - \overline{x}_{r(i_\beta-1)l})}{(\overline{x}_{ri_rl} - \overline{x}_{r(i_\beta-1)l})} \frac{(x_r - \overline{x}_{r(i_\beta+1)l})}{(\overline{x}_{ri_rl} - \overline{x}_{r(i_\beta+1)l})} \cdots \frac{(x_r - \overline{x}_{r\lambda_rl})}{(\overline{x}_{ri_rl} - \overline{x}_{r\lambda_rl})},
\end{aligned}
\tag{31}
$$

where the $\overline{x}_{r1l}, ..., \overline{x}_{r\lambda_rl}$, $r = 1, ..., n$ are the values of the system state x_r selected for sampling in the corresponding region; x_r is a dimension of $\mathbf{x}$, and $\mathbf{x} \in \Theta_l$. It should be noted that the Lagrange basis function $v_{ri_rl}(x_r)$ only applies in the subdomain Θ_l. Meanwhile, when $\mathbf{x} \notin \Theta_l$, $v_{ri_rl}(x_r) = 0$.

The order of Lagrange basis function is related to the number of sample points, which can be different and equals to $\lambda_r - 1$ in each system state. Hence, the order of LMFs are $\prod_{r=1}^{n}(\lambda_r - 1)$. According to the property of Lagrange interpolation functions[39], the sum of Lagrange basis functions is equal to 1, that is $\sum_{i_r=1}^{\lambda_r} v_{ri_rl}(x_r) = 1$. Thus, we can get the property as follows:

$$\sum_{i_1=1}^{\lambda_1} v_{1i_1l}(x_1) \times \cdots \times \sum_{i_n=1}^{\lambda_n} v_{ni_nl}(x_n) = \sum_{i_1=1}^{\lambda_1} \cdots \sum_{i_n=1}^{\lambda_n} \prod_{r=1}^{n} v_{ri_rl}(x_r) = 1. \tag{32}$$

Remark 6. For the LMFs (30), different sample points will lead to different approximation errors. In this paper, for each system state x_r, two endpoints are taken as the sample points, and then other sample points are selected by means of average distribution. In a fixed subdomain, smaller approximation errors require higher-order LMFs, but Runge phenomenon may occur as the order

of LMFs increases. To circumvent this problem, it is not appropriate to employ the high order LMFs in each fixed subdomain, but to increase the number of partitions appropriately.

Remark 7. For univariate LMFs, choosing Chebyshev nodes as sample points can obtain the same optimal polynomial approximated membership functions as CMFs, which can minimize the maximum absolute approximation errors. The design principle of Chebyshev nodes can refer to reference [30] in the revised paper. The calculation algorithm of Chebyshev nodes is:

$$\overline{x}_{1i_1 l} = \left(\frac{\overline{s} + \underline{s}}{2}\right) + \frac{\overline{s} - \underline{s}}{2}\cos\frac{2i_1 - 1}{2\lambda_1}\pi, i_1 = 1, ..., \lambda_1, \tag{33}$$

where $\underline{s}$ is the lower bound of subdomain; $\overline{s}$ is the upper bound of subdomain; λ_1 is the number of sample points in a subdomain and can be given different value for different subdomain; l is the index of the subdomain.

For multivariate LMFs, the average grid can be selected as the sample point to obtain the shape information of the membership function more comprehensively. Since there is no Chebyshev node of multiple LMF, it is not recommended to select many sample points in the subdomain to avoid the Ronge's phenomenon. The calculation algorithm of average grid points is:

$$\overline{x}_{ri_r l} = \left\{\left(\underline{s} + \frac{(i_1 - 1)(\overline{s} - \underline{s})}{\lambda_1 - 1}\right), \left(\underline{s} + \frac{(i_2 - 1)(\overline{s} - \underline{s})}{\lambda_2 - 1}\right), \cdots, \left(\underline{s} + \frac{(i_n - 1)(\overline{s} - \underline{s})}{\lambda_n - 1}\right)\right\}, \forall i_1, i_2, \cdots, i_n,$$

where $\lambda_1, \lambda_2, \cdots, \lambda_n$ are the number of sample points in each system state $x_r, r = 1, \cdots, n$, respectively, and can be given different value for different subdomain; $i_1 \in \{1, \cdots, \lambda_1\}, i_2 \in \{1, \cdots, \lambda_2\}, \cdots, i_n \in \{1, \cdots, \lambda_n\}$ are the index of the sample points on each system state; $\underline{s}$ is the lower bound of subdomain; $\overline{s}$ is the upper bound of subdomain; l is the index of the subdomain.

Remark 8. In a subdomain, when only two endpoints are taken as sample points on each system state x_r, we can get $\lambda_1 = \cdots = \lambda_n = 2$, and the LMFs (30) will be reduced to PLMFs[33], which are

$$\hat{h}_{ijl}(\mathbf{x}) = \sum_{i_1=1}^{2} \cdots \sum_{i_n=1}^{2} \prod_{r=1}^{n} v_{ri_r l}(x_r)\overline{h}_{iji_1 \cdots i_n l}, \tag{34}$$

where $\overline{h}_{iji_1 \cdots i_n l}$ is a constant; $v_{ri_r l}(x_r)$ are $\frac{x_r - \overline{x}_{r2l}}{\overline{x}_{r1l} - \overline{x}_{r2l}}$ and $\frac{x_r - \overline{x}_{r1l}}{\overline{x}_{r2l} - \overline{x}_{r1l}}$, where $\overline{x}_{r1l}$ and $\overline{x}_{r2l}$ are the two endpoints of $\mathbf{x}$ selected for sampling. Here, the $v_{ri_r l}(x_r)$ of LMFs and PLMFs are identical.

Furthermore, when two endpoints are taken as sample points on each system state x_r and the sample points $\overline{h}_{iji_1 \cdots i_n}$ turn to Taylor series expansion $\delta_{iji_1 \cdots i_n l}(\mathbf{x})$, the LMFs (30) will be converted to the TSMFs[34], which are

$$\hat{h}_{ijl}(\mathbf{x}) = \sum_{i_1=1}^{2} \cdots \sum_{i_n=1}^{2} \prod_{r=1}^{n} v_{ri_r l}(x_r)\delta_{iji_1 \cdots i_n l}(\mathbf{x}), \tag{35}$$

where $\delta_{iji_1 \cdots i_n l}(\mathbf{x})$ is the Taylor expansion at the sample points, and its order is determined by users. $v_{ri_r l}(x_r)$ are $\frac{x_r - \overline{x}_{r2l}}{\overline{x}_{r1l} - \overline{x}_{r2l}}$ and $\frac{x_r - \overline{x}_{r1l}}{\overline{x}_{r2l} - \overline{x}_{r1l}}$, where $\overline{x}_{r1l}$ and $\overline{x}_{r2l}$ are the two endpoints of $\mathbf{x}$ selected for sampling.

For different approximate membership function methods, Table 1 shows the type of MGI terms incorporated into the stability conditions, the selection approach of sample points in each subdomain, and the number of stability conditions including MGI terms.

TABLE 1 Comparison of different approximate membership functions

method	Terms	sample points	No. of conditions
PLMFs	$\overline{h}_{iji_1 \cdots i_n l}$	endpoints	$\prod_{r=1}^{n}(s_r + 1)$
PMFs	polynomial	none	$\prod_{r=1}^{n} s_r$
TSMFs	$\delta_{iji_1 \cdots i_n l}(\mathbf{x})$	endpoints	$\prod_{r=1}^{n}(s_r + 1)$
LMFs	polynomial	arbitrary	$\prod_{r=1}^{n} s_r$

From the Table 1, the number of stability conditions in LMFs is the same as that in PMFs, but less than that in PLMFs and TSMFs. In addition, the LMFs method can discretionarily select the number and location of sample points in each subdomain, thereby improving the capability of approximating the original membership functions.

Example 1. An example is considered to show the merits of LMFs method. We choose the membership function of control system as $h_{21}(\mathbf{x}) = w_2(\mathbf{x})m_1(\mathbf{y})$, where the membership function of model is $w_2(\mathbf{x}) = \frac{1}{1+e^{-(x_1+4)}} - \frac{1}{1+e^{-(x_1-4)}}$ and the membership function of controller is $m_1(\mathbf{y}) = e^{-x_1^2/12}$. Consider dividing the whole domain $x_1 \in [-10, 10]$ into five subdomains, which are $x_1 \in [-10, -6)$, $[-6, -2)$, $[-2, 2)$, $[2, 6)$ and $[6, 10]$. For each subdomain, we use PLMF[33], TSMF[34] and LMF methods to obtain the approximate membership function. To further illustrate the difference between LMF and PLMF, TSMF method, we take a subdomain $x_1 \in [6, 10]$ as an example, where l is 5. In this subdomain, only 6 and 10 are choose to construct the PLMF or TSMF, while for LMF, we can choose more sample points, for example, 6, 8 and 10 are selected for sampling according to the Remark 6. The approximate function $\hat{h}_{215}(x_1)$ is obtained by LMFs (30), and we have

$$\hat{h}_{215}(x_1) = v_{115}(x_1) \times h_{21}(6) + v_{125}(x_1) \times h_{21}(8) + v_{135}(x_1) \times h_{21}(10)$$
$$= 0.0007199x_1^2 - 0.013x_1 + 0.05803, \tag{36}$$

where $v_{115}(x_1) = \frac{(x_1-8)(x_1-10)}{(6-8)(6-10)}$, $v_{125}(x_1) = \frac{(x_1-6)(x_1-10)}{(8-6)(8-10)}$ and $v_{135}(x_1) = \frac{(x_1-6)(x_1-8)}{(10-6)(10-8)}$ are the Lagrange basis functions.

Besides, we chose the order of the TSMF is 2, so that we can compare the approximation capability with LMF in the same order. Table 2 gives the details of LMFs obtained by (30). The comparison for using different approximate membership function methods are shown in Fig. 2.

TABLE 2 Lagrange membership functions in different subdomain

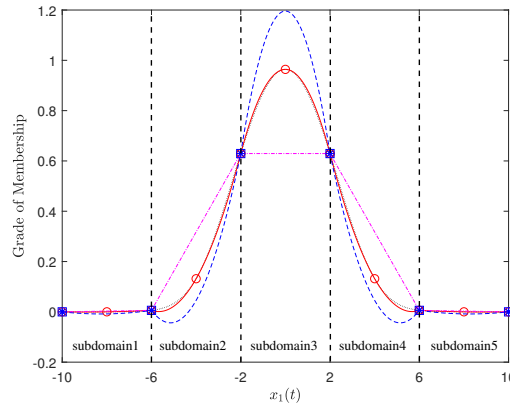| Subdomain	LMF
$[-10, -6)$	$0.0007199x_1^2 + 0.013x_1 + 0.05803$
$[-6, -2)$	$0.04648x_1^2 + 0.5277x_1 + 1.499$
$[-2, 2)$	$0.964 - 0.08367x_1^2$
$[2, 6)$	$0.04648x_1^2 - 0.5277x_1 + 1.499$
$[6, 10]$	$0.0007199x_1^2 - 0.013x_1 + 0.05803$

FIGURE 2 Solid line: LMF; Dashed line: TSMF; Dash-dot line: PLMF; Dotted line: original membership function; The sample points of LMF are indicated by "∘" and the sample points of PLMF and TSMF are indicated by "∗" and "□", respectively.

From Fig. 2, in the same subdomain, since more sample points can be interpolated into the LMFs, the capability of LMFs approximating the original membership functions can be higher than that of PLMFs and TSMFs, so that more membership information is employed to obtain the relaxed stability results.

Example 2. We use another example to show the proposed LMFs (30) can also be applied to approximate multi-variable membership functions. We consider the system states $\mathbf{x} = [x_1, x_2]$. The original membership function is $h_{21}(\mathbf{x}) = w_2(\mathbf{x})m_1(\mathbf{y})$, where the membership function of model is $w_2(\mathbf{x}) = \frac{1}{1+e^{-(x_1+4)}} - \frac{1}{1+e^{-(x_1-4)}}$ and the membership function of controller is $m_1(\mathbf{y}) =$

$e^{-(x_1+x_2)^2/12}$. The approximation result of LMF in the subdomains $x_1 \in [-2, 2]$ and $x_2 \in [-1, 1]$ is shown in Fig. 3. We select
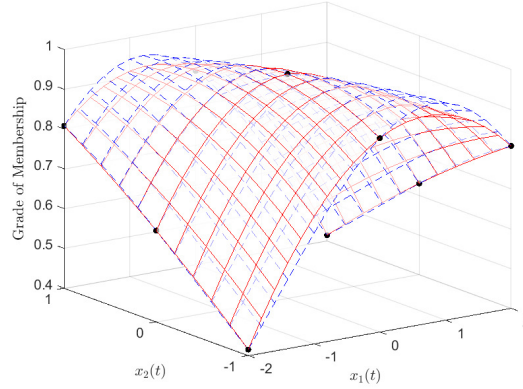

FIGURE 3 The plane of solid lines: original membership function. The plane of dashed lines: LMF. The sample points of LMF are indicated by "●".

the sample points $\{-2, 0, 2\}$ on x_1 and $\{-1, 0, 1\}$ on x_2, and then we can get the LMFs $h_{21}(\mathbf{x}) = 0.01481x_1^2x_2^2 - 0.08367x_1^2 - 0.0983x_1x_2 - 0.07708x_2^2 + 0.964$. Furthermore, to facilitate the calculation efficiency of the stability conditions, we can delete the terms whose coefficients are less than 10^{-10} through the interpolation method of LMFs. It can be concluded from Fig. 3 that the original multi-variable membership function can also be effectively obtained by the LMFs method.

4 | SIMULATION EXAMPLE

In the following, we provide a simulation example of SOF PFMB control system to demonstrate the validity of the proposed stability conditions in the Theorem 1 and Theorem 2. The system states of the SOF PFMB control system are $\hat{\mathbf{x}} = \mathbf{x} = [x_1 \ x_2]^T$. The original nonlinear system is provided as

$$\mathbf{A}_1(x_1) = \begin{bmatrix} 0.59 - 0.05x_1^2 & -7.29 - 0.01x_1 \\ 0.01 & -2.85 \end{bmatrix}, \mathbf{A}_2(x_1) = \begin{bmatrix} 1.02 - 0.25x_1^2 & -4.64 + 0.92x_1 \\ 0.35 & -8.56 \end{bmatrix},$$

$$\mathbf{A}_3(x_1) = \begin{bmatrix} -a - 0.15x_1^2 & -0.5 \\ -5.01 & -1.16 - 0.17x_1^2 \end{bmatrix}, \mathbf{B}_1(x_1) = \begin{bmatrix} 1 + 1.62x_1 \\ 1 \end{bmatrix}, \mathbf{B}_2(x_1) = \begin{bmatrix} 10 + 1.47x_1 \\ 0 \end{bmatrix},$$

$$\mathbf{B}_3(x_1) = \begin{bmatrix} -b + 0.02x_1 \\ -1 \end{bmatrix}, \mathbf{C} = [1 \quad 0],$$

where a and b are constants to facilitate the comparison of the conservativeness of different stability conditions. According to Lemma 1, the output matrix $\mathbf{C}$ offers $\mathbf{\Gamma} = \begin{bmatrix} 1 & 0 \\ 0 & 1 \end{bmatrix}$.

For the polynomial fuzzy model, the membership functions are $w_1(\mathbf{x}) = 1 - \frac{1}{1+e^{-(x_1+4)}}$, $w_2(\mathbf{x}) = 1 - w_1(x_1) - w_3(x_1)$ and $w_3(\mathbf{x}) = \frac{1}{1+e^{-(x_1-4)}}$. For the polynomial fuzzy controllers, the membership functions are designed as $m_1(\mathbf{y}) = e^{-x_1^2/12}$ and $m_2(\mathbf{y}) = 1 - m_1(\mathbf{y})$ under the IPM design concept.

Next, three scenarios is to show the difference between the stability conditions of the Theorem 1 and Theorem 2 in relaxation stability analysis.

1) Based on the membership grade non-integration (MGN) method, the stabilization region obtained by the Theorem 1 is a baseline for comparison with other approaches.
2) The influence of the LMFs in Theorem 2 under different orders and subdomains on the size of stabilization region.
3) The influence of the number of subdomains, the order of LMFs and the order of slack matrices $\mathbf{M}_l(\mathbf{x})$ in Theorem 2 on the size of the stabilization region.

In the first scenario, we employ the Theorem 1 to investigate the stability of SOF PFMB control system. We choose $\mathbf{P}(\tilde{\mathbf{x}})$ as 0 degree, $\mathbf{N}_j(\mathbf{x})$ as 0 to 2 degrees, and use the SOSTOOLs to obtain the stabilization region, however, the result shows that there is no stabilization region since Theorem 1 not contains the membership information and/or premise variables.

In terms of the second scenario, the Theorem 2 was employed to investigate the stabilization region by setting different LMFs. In order to demonstrate the order of LMFs and the number of partitions can influence the stabilization regions, we consider different settings as shown in Table 3.

TABLE 3 Different order and subdomain settings of LMFs

Case	Order of LMFs	Partitions	Points of Partitions
1	1	4	$\{-10, -5, 0, 5, 10\}$
2	3	4	$\{-10, -5, 0, 5, 10\}$
3	1	10	$\{-10, -8, ..., 8, 10\}$
4	3	10	$\{-10, -8, ..., 8, 10\}$

The LMFs are obtained by (30) with the settings in Table 3. By designing the LMFs in each subdomain, the upper bound of absolute value of approximation error $\overline{\gamma}_{ij}$ is given in Tables 4-7.

TABLE 4 upper bound of absolute value of approximation error $\overline{\gamma}_{ij}$ in Case 1, Case 5 and Case 6

subdomains	$\overline{\gamma}_{ij}$		
$[-10, -5)$	$\overline{\gamma}_{11} = 3.866 \times 10^{-2}$,	$\overline{\gamma}_{12} = 1.541 \times 10^{-1}$,	$\overline{\gamma}_{21} = 2.143 \times 10^{-2}$
	$\overline{\gamma}_{22} = 9.571 \times 10^{-2}$,	$\overline{\gamma}_{31} = 1.016 \times 10^{-5}$,	$\overline{\gamma}_{32} = 4.957 \times 10^{-5}$
$[-5, 0)$	$\overline{\gamma}_{11} = 6.771 \times 10^{-2}$,	$\overline{\gamma}_{12} = 2.481 \times 10^{-1}$,	$\overline{\gamma}_{21} = 9.244 \times 10^{-2}$
	$\overline{\gamma}_{22} = 2.454 \times 10^{-1}$,	$\overline{\gamma}_{31} = 9.262 \times 10^{-3}$,	$\overline{\gamma}_{32} = 6.770 \times 10^{-4}$
$[0, 5)$	$\overline{\gamma}_{11} = 9.262 \times 10^{-3}$,	$\overline{\gamma}_{12} = 6.770 \times 10^{-4}$,	$\overline{\gamma}_{21} = 9.244 \times 10^{-2}$
	$\overline{\gamma}_{22} = 2.454 \times 10^{-1}$,	$\overline{\gamma}_{31} = 6.771 \times 10^{-2}$,	$\overline{\gamma}_{32} = 2.481 \times 10^{-1}$
$[5, 10]$	$\overline{\gamma}_{11} = 1.016 \times 10^{-5}$,	$\overline{\gamma}_{12} = 4.957 \times 10^{-5}$,	$\overline{\gamma}_{21} = 2.143 \times 10^{-2}$
	$\overline{\gamma}_{22} = 9.571 \times 10^{-2}$,	$\overline{\gamma}_{31} = 3.866 \times 10^{-2}$,	$\overline{\gamma}_{32} = 1.541 \times 10^{-1}$

TABLE 5 upper bound of absolute value of approximation error $\overline{\gamma}_{ij}$ in Case 2

subdomains	$\overline{\gamma}_{ij}$		
$[-10, -5)$	$\overline{\gamma}_{11} = 1.971 \times 10^{-3}$,	$\overline{\gamma}_{12} = 4.504 \times 10^{-3}$,	$\overline{\gamma}_{21} = 4.396 \times 10^{-3}$
	$\overline{\gamma}_{22} = 2.271 \times 10^{-3}$,	$\overline{\gamma}_{31} = 2.605 \times 10^{-6}$,	$\overline{\gamma}_{32} = 3.566 \times 10^{-6}$
$[-5, 0)$	$\overline{\gamma}_{11} = 7.358 \times 10^{-3}$,	$\overline{\gamma}_{12} = 2.981 \times 10^{-2}$,	$\overline{\gamma}_{21} = 1.906 \times 10^{-2}$
	$\overline{\gamma}_{22} = 4.114 \times 10^{-2}$,	$\overline{\gamma}_{31} = 7.032 \times 10^{-4}$,	$\overline{\gamma}_{32} = 1.614 \times 10^{-4}$
$[0, 5)$	$\overline{\gamma}_{11} = 7.032 \times 10^{-4}$,	$\overline{\gamma}_{12} = 1.614 \times 10^{-4}$,	$\overline{\gamma}_{21} = 1.906 \times 10^{-2}$
	$\overline{\gamma}_{22} = 4.114 \times 10^{-2}$,	$\overline{\gamma}_{31} = 7.358 \times 10^{-3}$,	$\overline{\gamma}_{32} = 2.981 \times 10^{-2}$
$[5, 10]$	$\overline{\gamma}_{11} = 2.605 \times 10^{-6}$,	$\overline{\gamma}_{12} = 3.566 \times 10^{-6}$,	$\overline{\gamma}_{21} = 4.396 \times 10^{-3}$
	$\overline{\gamma}_{22} = 2.271 \times 10^{-3}$,	$\overline{\gamma}_{31} = 1.971 \times 10^{-3}$,	$\overline{\gamma}_{32} = 4.504 \times 10^{-3}$

Referring to Theorem 2, the values of $\iota_1(\tilde{\mathbf{x}})$, $\iota_2(\tilde{\mathbf{x}})$, $\iota_3(\tilde{\mathbf{x}})$, $\iota_4(\tilde{\mathbf{x}})$ and $\iota_5(\tilde{\mathbf{x}})$ are chosen as 1×10^{-3}. $\mathbf{P}(\tilde{\mathbf{x}})$ is chosen as 0 degree; $\mathbf{Y}_{ijl}(\mathbf{x})$ and $\mathbf{M}_l(\mathbf{x})$ both are chosen together 0, 2 and 4 degrees; $\mathbf{N}_j(\mathbf{x})$ is chosen from 0 to 2 degrees. Moreover, to reduce the

computational complexity, $\mathbf{Y}_{ij}(\mathbf{x})$ and $\mathbf{M}(\mathbf{x})$ with the same order are employed instead of $\mathbf{Y}_{ijl}(\mathbf{x})$ and $\mathbf{M}_l(\mathbf{x})$. Based on the Theorem 2 and the parameter settings in Table 3, the obtained stabilization region is shown in Fig. 4.

T A B L E 6 upper bound of absolute value of approximation error $\overline{\gamma}_{ij}$ in Case 3, Case 7 and Case 8

subdomains	$\overline{\gamma}_{ij}$
$[-10, -8)$	$\overline{\gamma}_{11} = 1.378 \times 10^{-3}, \quad \overline{\gamma}_{12} = 5.002 \times 10^{-3}, \quad \overline{\gamma}_{21} = 4.025 \times 10^{-5}$ $\overline{\gamma}_{22} = 3.585 \times 10^{-3}, \quad \overline{\gamma}_{31} = 1.380 \times 10^{-8}, \quad \overline{\gamma}_{32} = 1.247 \times 10^{-6}$
$[-8, -6)$	$\overline{\gamma}_{11} = 8.318 \times 10^{-3}, \quad \overline{\gamma}_{12} = 2.982 \times 10^{-2}, \quad \overline{\gamma}_{21} = 2.394 \times 10^{-3}$ $\overline{\gamma}_{22} = 1.917 \times 10^{-2}, \quad \overline{\gamma}_{31} = 9.445 \times 10^{-7}, \quad \overline{\gamma}_{32} = 8.387 \times 10^{-6}$
$[-6, -4)$	$\overline{\gamma}_{11} = 5.351 \times 10^{-3}, \quad \overline{\gamma}_{12} = 3.848 \times 10^{-2}, \quad \overline{\gamma}_{21} = 3.610 \times 10^{-2}$ $\overline{\gamma}_{22} = 9.343 \times 10^{-3}, \quad \overline{\gamma}_{31} = 3.192 \times 10^{-5}, \quad \overline{\gamma}_{32} = 3.731 \times 10^{-5}$
$[-4, -2)$	$\overline{\gamma}_{11} = 1.889 \times 10^{-2}, \quad \overline{\gamma}_{12} = 5.909 \times 10^{-2}, \quad \overline{\gamma}_{21} = 3.716 \times 10^{-2}$ $\overline{\gamma}_{22} = 7.705 \times 10^{-2}, \quad \overline{\gamma}_{31} = 5.195 \times 10^{-4}, \quad \overline{\gamma}_{32} = 2.235 \times 10^{-5}$
$[-2, 0)$	$\overline{\gamma}_{11} = 8.074 \times 10^{-3}, \quad \overline{\gamma}_{12} = 1.379 \times 10^{-2}, \quad \overline{\gamma}_{21} = 7.412 \times 10^{-2}$ $\overline{\gamma}_{22} = 5.023 \times 10^{-2}, \quad \overline{\gamma}_{31} = 3.783 \times 10^{-3}, \quad \overline{\gamma}_{32} = 1.998 \times 10^{-4}$
$[0, 2)$	$\overline{\gamma}_{11} = 3.783 \times 10^{-3}, \quad \overline{\gamma}_{12} = 1.998 \times 10^{-4}, \quad \overline{\gamma}_{21} = 7.412 \times 10^{-2}$ $\overline{\gamma}_{22} = 5.023 \times 10^{-2}, \quad \overline{\gamma}_{31} = 8.074 \times 10^{-3}, \quad \overline{\gamma}_{32} = 1.379 \times 10^{-2}$
$[2, 4)$	$\overline{\gamma}_{11} = 5.195 \times 10^{-4}, \quad \overline{\gamma}_{12} = 2.235 \times 10^{-5}, \quad \overline{\gamma}_{21} = 3.716 \times 10^{-2}$ $\overline{\gamma}_{22} = 7.705 \times 10^{-2}, \quad \overline{\gamma}_{31} = 1.889 \times 10^{-2}, \quad \overline{\gamma}_{32} = 5.909 \times 10^{-2}$
$[4, 6)$	$\overline{\gamma}_{11} = 3.192 \times 10^{-5}, \quad \overline{\gamma}_{12} = 3.731 \times 10^{-5}, \quad \overline{\gamma}_{21} = 3.610 \times 10^{-2}$ $\overline{\gamma}_{22} = 9.343 \times 10^{-3}, \quad \overline{\gamma}_{31} = 5.351 \times 10^{-3}, \quad \overline{\gamma}_{32} = 3.848 \times 10^{-2}$
$[6, 8)$	$\overline{\gamma}_{11} = 9.445 \times 10^{-7}, \quad \overline{\gamma}_{12} = 8.387 \times 10^{-6}, \quad \overline{\gamma}_{21} = 2.394 \times 10^{-3}$ $\overline{\gamma}_{22} = 1.917 \times 10^{-2}, \quad \overline{\gamma}_{31} = 8.318 \times 10^{-3}, \quad \overline{\gamma}_{32} = 2.982 \times 10^{-2}$
$[8, 10]$	$\overline{\gamma}_{11} = 1.380 \times 10^{-8}, \quad \overline{\gamma}_{12} = 1.247 \times 10^{-6}, \quad \overline{\gamma}_{21} = 4.025 \times 10^{-5}$ $\overline{\gamma}_{22} = 3.585 \times 10^{-3}, \quad \overline{\gamma}_{31} = 1.378 \times 10^{-3}, \quad \overline{\gamma}_{32} = 5.002 \times 10^{-3}$

T A B L E 7 upper bound of absolute value of approximation error $\overline{\gamma}_{ij}$ in Case 4

| subdomains	$\overline{\gamma}_{ij}$
$[-10, -8)$	$\overline{\gamma}_{11} = 2.895 \times 10^{-5}, \quad \overline{\gamma}_{12} = 8.712 \times 10^{-5}, \quad \overline{\gamma}_{21} = 3.444 \times 10^{-6}$ $\overline{\gamma}_{22} = 5.471 \times 10^{-5}, \quad \overline{\gamma}_{31} = 1.205 \times 10^{-9}, \quad \overline{\gamma}_{32} = 2.136 \times 10^{-8}$
$[-8, -6)$	$\overline{\gamma}_{11} = 4.968 \times 10^{-5}, \quad \overline{\gamma}_{12} = 1.406 \times 10^{-4}, \quad \overline{\gamma}_{21} = 1.247 \times 10^{-4}$ $\overline{\gamma}_{22} = 6.414 \times 10^{-5}, \quad \overline{\gamma}_{31} = 6.004 \times 10^{-8}, \quad \overline{\gamma}_{32} = 1.067 \times 10^{-7}$
$[-6, -4)$	$\overline{\gamma}_{11} = 2.863 \times 10^{-4}, \quad \overline{\gamma}_{12} = 1.141 \times 10^{-3}, \quad \overline{\gamma}_{21} = 1.822 \times 10^{-4}$ $\overline{\gamma}_{22} = 1.036 \times 10^{-3}, \quad \overline{\gamma}_{31} = 1.335 \times 10^{-6}, \quad \overline{\gamma}_{32} = 1.086 \times 10^{-7}$
$[-4, -2)$	$\overline{\gamma}_{11} = 3.645 \times 10^{-4}, \quad \overline{\gamma}_{12} = 1.295 \times 10^{-3}, \quad \overline{\gamma}_{21} = 7.748 \times 10^{-4}$ $\overline{\gamma}_{22} = 1.700 \times 10^{-3}, \quad \overline{\gamma}_{31} = 1.173 \times 10^{-5}, \quad \overline{\gamma}_{32} = 2.809 \times 10^{-6}$
$[-2, 0)$	$\overline{\gamma}_{11} = 1.819 \times 10^{-4}, \quad \overline{\gamma}_{12} = 3.070 \times 10^{-4}, \quad \overline{\gamma}_{21} = 5.894 \times 10^{-4}$ $\overline{\gamma}_{22} = 7.925 \times 10^{-4}, \quad \overline{\gamma}_{31} = 2.304 \times 10^{-5}, \quad \overline{\gamma}_{32} = 3.889 \times 10^{-5}$
$[0, 2)$	$\overline{\gamma}_{11} = 2.304 \times 10^{-5}, \quad \overline{\gamma}_{12} = 3.889 \times 10^{-5}, \quad \overline{\gamma}_{21} = 5.894 \times 10^{-4}$ $\overline{\gamma}_{22} = 7.925 \times 10^{-4}, \quad \overline{\gamma}_{31} = 1.819 \times 10^{-4}, \quad \overline{\gamma}_{32} = 3.070 \times 10^{-4}$
$[2, 4)$	$\overline{\gamma}_{11} = 1.173 \times 10^{-5}, \quad \overline{\gamma}_{12} = 2.809 \times 10^{-6}, \quad \overline{\gamma}_{21} = 7.748 \times 10^{-4}$ $\overline{\gamma}_{22} = 1.700 \times 10^{-3}, \quad \overline{\gamma}_{31} = 3.645 \times 10^{-4}, \quad \overline{\gamma}_{32} = 1.295 \times 10^{-3}$
$[4, 6)$	$\overline{\gamma}_{11} = 1.335 \times 10^{-6}, \quad \overline{\gamma}_{12} = 1.086 \times 10^{-7}, \quad \overline{\gamma}_{21} = 1.822 \times 10^{-4}$ $\overline{\gamma}_{22} = 1.036 \times 10^{-3}, \quad \overline{\gamma}_{31} = 2.863 \times 10^{-4}, \quad \overline{\gamma}_{32} = 1.141 \times 10^{-3}$
$[6, 8)$	$\overline{\gamma}_{11} = 6.004 \times 10^{-8}, \quad \overline{\gamma}_{12} = 1.067 \times 10^{-7}, \quad \overline{\gamma}_{21} = 1.247 \times 10^{-4}$ $\overline{\gamma}_{22} = 6.414 \times 10^{-5}, \quad \overline{\gamma}_{31} = 4.968 \times 10^{-5}, \quad \overline{\gamma}_{32} = 1.406 \times 10^{-4}$
$[8, 10]$	$\overline{\gamma}_{11} = 1.205 \times 10^{-9}, \quad \overline{\gamma}_{12} = 2.136 \times 10^{-8} \quad \overline{\gamma}_{21} = 3.444 \times 10^{-6}$ $\overline{\gamma}_{22} = 5.471 \times 10^{-5} \quad \overline{\gamma}_{31} = 2.895 \times 10^{-5}, \quad \overline{\gamma}_{32} = 8.712 \times 10^{-5}$
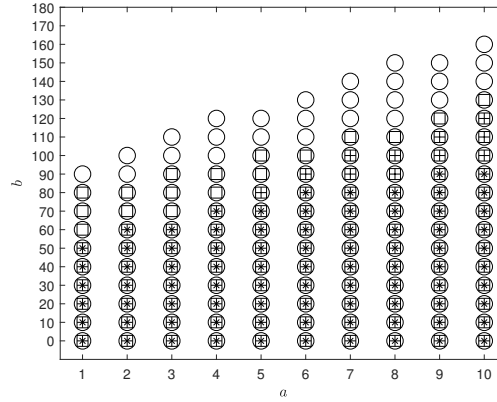
FIGURE 4 Combining the parameters in Table 3, stabilization regions are obtained and indicated by "×" for Case 1, "+" for Case 2, "□" for Case 3,"○" for Case 4, respectively.

From Fig. 4 for Case 1 and Case 2, the higher-order LMFs provide the larger stabilization region. This conclusion is consistent with the comparison of Case 3 and Case 4. On the other hand, compared with Case 1 and Case 3, more partitions provide a larger stabilization region. This conclusion is consistent with the comparison of Case 2 and Case 4. Therefore, in this example, it demonstrates that as the order of LMFs or the number of partitions increases, more and more membership information is brought into the stability conditions to achieve a larger stabilization region.

Next, we select some stable points on the boundary of the stabilization region and draw their phase plots to illustrate the correctness of the simulation results. For example, the stable points we choose for Case 1 are $a = 10$ and $b = 90$, and $\mathbf{G}_1(\mathbf{y}) = [-0.01692x_1^2 + 0.007173x_1 - 0.2368]$ and $\mathbf{G}_2(\mathbf{y}) = [0.009943x_1^2 + 0.008498x_1 - 0.05181]$; The stable points we choose for Case 2 are $a = 10$ and $b = 120$, and $\mathbf{G}_1(\mathbf{y}) = [0.005296x_1^2 - 0.003472x_1 - 0.1584]$ and $\mathbf{G}_2(\mathbf{y}) = [0.002509x_1^2 + 0.002225x_1 - 0.1042]$; The stable points we choose for Case 3 are $a = 10$ and $b = 130$, and $\mathbf{G}_1(\mathbf{y}) = [0.01197x_1^2 - 0.002132x_1 - 0.1659]$ and $\mathbf{G}_2(\mathbf{y}) = [0.01204x_1^2 - 0.002735x_1 - 0.09658]$; The stable points we choose for Case 4 are $a = 10$ and $b = 160$, and $\mathbf{G}_1(\mathbf{y}) = [0.01017x_1^2 - 0.009294x_1 - 0.1579]$ and $\mathbf{G}_2(\mathbf{y}) = [0.005108x_1^2 - 0.002238x_1 - 0.086]$. The corresponding phase plots are obtained as shown in Fig. 5. From all the phase plots, it can be concluded that the SOF polynomial fuzzy controllers designed in this paper can successfully stabilize the polynomial fuzzy system.

For the last scenario, the influence of the order of slack matrices $\mathbf{M}_l(\mathbf{x})$ on the stabilization region is investigated. The following comparison is made as shown in Table 8.

TABLE 8 Different order and subdomain settings of $\mathbf{M}_l(\mathbf{x})$

Case	Order of $\mathbf{M}_l(\mathbf{x})$	Partitions	Points of Partitions
5	2	4	{−10, −5, 0, 5, 10}
6	4	4	{−10, −5, 0, 5, 10}
7	2	10	{−10, −8, ..., 8, 10}
8	4	10	{−10, −8, ..., 8, 10}

The LMFs are designed as first-order polynomial functions, which are obtained by (30). The partition settings of LMFs are set in Table 8. $\overline{\gamma}_{ij}$ can be achieved by LMFs designed in each subdomain, and is given in Tables 4 and 6.

$\mathbf{Y}_{ij}(\mathbf{x})$ and $\mathbf{M}(\mathbf{x})$ are employed to alleviate the computational burden. Meanwhile, according to the settings in Table 8, we further set that when the order of $\mathbf{M}(\mathbf{x})$ is 2, only 0 and 2 terms are included, and when the order of $\mathbf{M}(\mathbf{x})$ is 4, only 0, 2 and 4 terms are included. The other parameters are chosen as discussed in scenario 2. By applying the above settings to Theorem 2, the stabilization region is achieved and shown in Fig. 6.

By comparing the stabilization regions under Case 5 and Case 6 in Fig. 6, we can draw the conclusion that the higher the order of slack matrices $\mathbf{M}_l(\mathbf{x})$, the larger the stabilization region. This is consistent with the comparison between Case 7 and Case 8. The slack matrix $\mathbf{M}_l(\mathbf{x})$ with higher-order can introduce more regional information of premise variables to achieve the relaxed stability conditions.
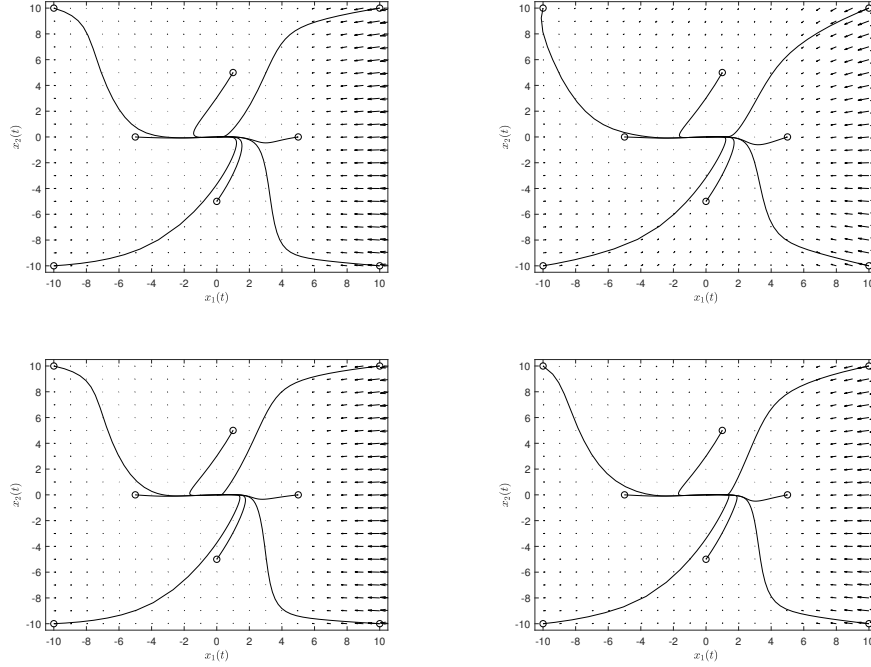
FIGURE 5 Top left phase plots are $a = 10$ and $b = 90$ (stabilization regions indicated by the symbols "$\times$"), the top right phase plots are $a = 10$ and $b = 120$ (stability region indicated by the symbols "+"). The bottom left phase plots are $a = 10$ and $b = 130$ (stabilization regions indicated by the symbols "$\square$"), the bottom right phase plots are $a = 10$ and $b = 160$ (stability region indicated by the symbols "$\circ$") all referring to Fig. 4.
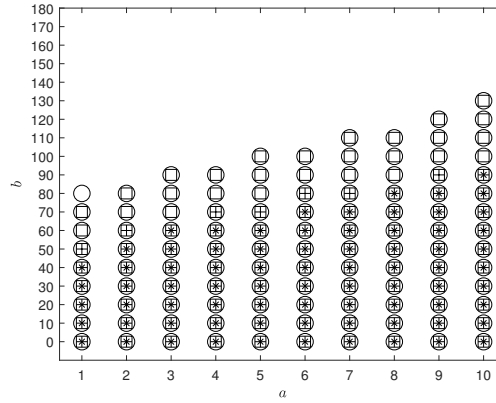

FIGURE 6 Combining the parameters in Table 8, stabilization regions are obtained and indicated by "$\times$" for Case 5, "+" for Case 6, "$\square$" for Case 7, "$\circ$" for Case 8, respectively.

Next, we select some stable points on the boundary of the stabilization region and draw their phase plots to illustrate the correctness of the simulation results. For example, the stable points we choose for Case 5 are $a = 9$ and $b = 80$, and the feedback gains $\mathbf{G}_j(\mathbf{y})$ are $\mathbf{G}_1(\mathbf{y}) = [-0.003941x_1{}^2 + 0.03958x_1 - 0.2363]$ and $\mathbf{G}_2(\mathbf{y}) = [0.004184x_1{}^2 + 0.003147x_1 - 0.02939]$; The stable points we choose for Case 6 are $a = 9$ and $b = 90$, and the feedback gains $\mathbf{G}_j(\mathbf{y})$ are $\mathbf{G}_1(\mathbf{y}) = [-0.006518x_1{}^2 + 0.03247x_1 - 0.3616]$ and $\mathbf{G}_2(\mathbf{y}) = [0.002878x_1{}^2 + 0.003782x_1 + 0.004202]$; The stable points we choose for Case 7 are $a = 1$ and $b = 70$, and the feedback gains $\mathbf{G}_j(\mathbf{y})$ are $\mathbf{G}_1(\mathbf{y}) = [0.001915x_1{}^2 + 0.001635x_1 - 0.2031]$ and $\mathbf{G}_2(\mathbf{y}) = [0.01655x_1{}^2 - 0.001867x_1 - 0.07937]$; The stable points we choose for Case 8 are $a = 1$ and $b = 80$, and the feedback gains $\mathbf{G}_j(\mathbf{y})$ are $\mathbf{G}_1(\mathbf{y}) = [0.03448x_1{}^2 - 0.0002243x_1 -$
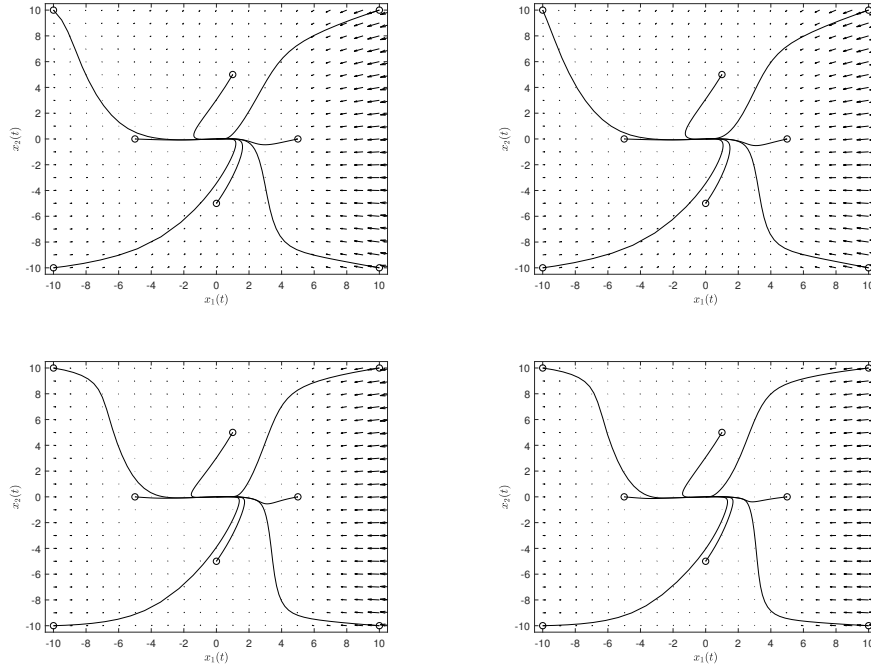
FIGURE 7 The top left phase plots are $a = 9$ and $b = 80$ (stabilization regions indicated by the symbols "×"), the top right phase plots are $a = 9$ and $b = 90$ (stability region indicated by the symbols "+"). The bottom left phase plots are $a = 1$ and $b = 70$ (stabilization regions indicated by the symbols "□"), the bottom right phase plots are $a = 1$ and $b = 80$ (stability region indicated by the symbols "○") all referring to Fig. 6.

0.3343] and $\mathbf{G}_2(\mathbf{y}) = [0.01968x_1{}^2 - 0.000006x_1 - 0.07016]$. The corresponding phase plots are obtained as shown in Fig. 7 which can be concluded that the SOF polynomial fuzzy controllers designed in this paper can successfully stabilize the polynomial fuzzy system.

5 | CONCLUSION

This paper designed a novel MGI technique to investigate the stabilization control problem for the SOF PFMB control system under the IPM concept. Through the nonsingular transformation matrix and the diagonal positive-definite Lyapunov matrix, the non-convex constraint of the stability conditions has been solved. Furthermore, the original membership functions are approximated with LMFs which can achieve the relaxed stability analysis results. One of the advantages of LMFs method is that it is an extension of PLMFs, which can employ more sample points to improve the approximation capability. Another advantage of the LMFs method is that it can be regarded as a general representation of PMFs method, and can be used as the specific implementation method of the basic functions of CMFs method. Combining the LMFs and premise variables into a novel MGI method can further relax the stability conditions. Finally, we use a simulation example to validate the advantages of the proposed stability analysis results.

REFERENCES

1. Lam HK. *Polynomial Fuzzy Model-Based Control Systems*. Springer, 2016.
2. Syrmos VL, Abdallah CT, Dorato P, Grigoriadis K. Static output feedback- A survey. *Automatica*. 1997;33(2):125-137.
3. Ghaoui LE, Oustry F, Aitrami M. A cone complementarity linearization algorithm for static output-feedback and related problems. *IEEE Transactions on Automatic Control*. 1997;42(8):1171-1176.
4. Gao H, Wang Z, Wang C. Improved H_∞ control of discrete-time fuzzy systems: A cone complementarity linearization approach.. *Information Sciences*. 2005;175(1):57-77.
5. Sun TX. Static Output Feedback Stabilization: An ILMI Approach. *Automatica*. 1998;34(12):1641-1645.
6. Wu HN, Zhang HY. Reliable mixed $L2/H_\infty$ fuzzy static output feedback control for nonlinear systems with sensor faults. *Automatica*. 2005;41(11):1925-1932.

7. Geromel JC, Souza CCD, Skelton RE. Static output feedback controllers: Stability and convexity. *IEEE Transactions on Automatic Control*. 1998;43(1):120-125.

8. Lo JC, Lin ML. Robust H_∞, Nonlinear Control via Fuzzy Static Output Feedback. *IEEE Transactions on Circuits & Systems I Fundamental Theory & Applications*. 2003;50(11):1494-1502.

9. Crusius CAR, Trofino A. Sufficient LMI condition for output feedback control problems. *IEEE Transactions on Automatic Control*. 1999;44(5):1053-1057.

10. Nachidi M, Benzaouia A, Tadeo F, Rami MA. LMI-based Approach for Output-Feedback Stabilization for Discrete-Time Takagi–Sugeno Systems. *IEEE Transactions on Fuzzy Systems*. 2008;16(5):1188-1196.

11. Soliman M, Elshafei AL, Bendary F, Mansour W. LMI static output-feedback design of fuzzy power system stabilizers. *Expert Systems with Applications*. 2009;36(3):6817-6825.

12. Sugeno M, Kang GT. Structure identification of fuzzy model. *Fuzzy Sets & Systems*. 1988;28(1):15-33.

13. Takagi T, Sugeno M. Fuzzy identification of systems and its applications to modeling and control. *Readings in Fuzzy Sets for Intelligent Systems*. 1993;15(1):387-403.

14. Kau SW, Lee HJ, Yang CM, Lee CH, Hong L, Fang CH. Robust fuzzy static output feedback control of T-S fuzzy systems with parametric uncertainties. *Fuzzy Sets and Systems*. 2007;158(2):135-146. doi: 10.1016/j.fss.2006.09.010

15. Jeung ET, Lee KR. Static output feedback control for continuous-time T-S fuzzy systems: An LMI approach. *International Journal of Control Automation & Systems*. 2014;12(3):703-708.

16. Qiu J, Gang F, Gao H. Static-Output-Feedback Control of Continuous-Time T-S Fuzzy Affine Systems Via Piecewise Lyapunov Functions. *IEEE Transactions on Fuzzy Systems*. 2013;21(2):245-261.

17. Tanaka K, Yoshida H, Ohtake H, Wang HO. A Sum-of-Squares Approach to Modeling and Control of Nonlinear Dynamical Systems With Polynomial Fuzzy Systems. *IEEE Transactions on Fuzzy Systems*. 2009;17(4):911-922.

18. Tanaka K, Ohtake H, Seo T, Tanaka M, Wang HO. Polynomial Fuzzy Observer Designs: A Sum-of-Squares Approach. *IEEE Transactions on Systems, Man, and Cybernetics, Part B (Cybernetics)*. 2012;42(5):1330-1342.

19. Meng A, Lam HK, Yan Y, Li X, Liu F. Static Output Feedback Stabilization of Positive Polynomial Fuzzy Systems. *IEEE Transactions on Fuzzy Systems*. 2018;26(3):1600-1612.

20. Meng A, Lam H, Liu F, Zhang C, Qi P. Output Feedback and Stability Analysis of Positive Polynomial Fuzzy Systems. *IEEE Transactions on Systems, Man, and Cybernetics: Systems*. 2020:1-12.

21. Lo JC, Liu JW. Polynomial static output feedback H_∞ control via homogeneous Lyapunov functions. *International Journal of Robust and Nonlinear Control*. 2019;29(6):1639-1659. doi: 10.1002/rnc.4451

22. Lam HK, Wu L, Lam J. Two-Step Stability Analysis for General Polynomial-Fuzzy-Model-Based Control Systems. *IEEE Transactions on Fuzzy Systems*. 2015;23(3):511-524.

23. Dong Y, Song Y, Wang J, Zhang B. Dynamic output-feedback fuzzy MPC for Takagi-Sugeno fuzzy systems under event-triggering–based try-once-discard protocol. *International Journal of Robust and Nonlinear Control*. 2019;30(4):1394-1416. doi: 10.1002/rnc.4816

24. Lam HK, Narimani M. Stability analysis and performance design for fuzzy-model-based control system under imperfect premise matching. *IEEE Transactions on Fuzzy Systems*. 2008;17(4):949–961.

25. Li X, Lam HK, Ge S, Liu F. Stability Analysis of Positive Polynomial Fuzzy-Model-Based Control Systems with Time Delay under Imperfect Premise Matching. *IEEE Transactions on Fuzzy Systems*. 2018;26(4):2289-2300.

26. Lam HK, Leung FHF. Stability analysis of fuzzy control systems subject to uncertain grades of membership. *IEEE Transactions on Systems, Man, and Cybernetics, Part B (Cybernetics)*. 2005;35(6):1322-1325.

27. Fan X, Wang Z. Event-triggered integral sliding mode control for fractional order T-S fuzzy systems via a fuzzy error function. *International Journal of Robust and Nonlinear Control*. 2021;31(7):2491-2508. doi: 10.1002/rnc.5400

28. Lam HK. Stability Analysis of Polynomial Fuzzy Model Based Control Systems with Mismatched Premise Membership Functions Through Symbolic Variables. *IEEE Transactions on Fuzzy Systems*. 2014;22(1):223-229.

29. Li X, Lam HK, Liu F, Zhao X. Stability and Stabilization Analysis of Positive Polynomial Fuzzy Systems with Time Delay Considering Piecewise Membership Functions. *IEEE Transactions on Fuzzy Systems*. 2017;25(4):958-971.

30. Narimani M, Lam HK. SOS-Based Stability Analysis of Polynomial Fuzzy-Model-Based Control Systems Via Polynomial Membership Functions. *IEEE Transactions on Fuzzy Systems*. 2010;18(5):862-871.

31. Narimani M, Lam HK, Dilmaghani R, Wolfe C. LMI-based Stability Analysis of Fuzzy-Model-Based Control Systems Using Approximated Polynomial Membership Functions. *IEEE Transactions on Systems, Man, and Cybernetics, Part B (Cybernetics)*. 2011;41(3):713-724.

32. Bao Z, Li X, Lam HK, Peng Y, Liu F. Membership-Function-Dependent Stability Analysis for Polynomial Fuzzy-Model-Based Control Systems via Chebyshev Membership Functions. *IEEE Transactions on Fuzzy Systems*. 2020:1-1. doi: 10.1109/TFUZZ.2020.3018185

33. Lam HK. Polynomial Fuzzy-Model-Based Control Systems: Stability Analysis Via Piecewise-Linear Membership Functions. *IEEE Transactions on Fuzzy Systems*. 2011;19(3):588-593.

34. Lam HK, Liu C, Wu L, Zhao X. Polynomial fuzzy-model-based control systems: Stability analysis via approximated membership functions considering sector nonlinearity of control input. *IEEE Transactions on Fuzzy Systems*. 2015;23(6):2202-2214.

35. Li X, Mehran K, Bao Z. Stability Analysis of Discrete-Time Polynomial Fuzzy-Model-Based Control Systems With Time Delay and Positivity Constraints Through Piecewise Taylor Series Membership Functions. *IEEE Transactions on Systems, Man, and Cybernetics: Systems*. 2020(99):1-13. doi: 10.1109/TSMC.2020.2969095.

36. Lam HK. A review on stability analysis of continuous-time fuzzy-model-based control systems: From membership-function-independent to membership-function-dependent analysis. *Engineering Applications of Artificial Intelligence*. 2018;68:390-408. doi: 10.1016/j.engappai.2017.09.007

37. Li X, Mehran K. Model-Based Control and Stability Analysis of Discrete-Time Polynomial Fuzzy Systems With Time Delay and Positivity Constraints. *IEEE Transactions on Fuzzy Systems*. 2019;27(11):2090-2100.

38. Li X, Mehran K, Lam HK, Xiao B, Bao Z. Stability analysis of discrete-time positive polynomial-fuzzy-model-based control systems through fuzzy co-positive Lyapunov function with bounded control. *IET Control Theory Applications*. 2020;14(2):233-243.

39. Sauer T. *Numerical Analysis*. China Machine Press, 2012.

40. Lam HK. Output-feedback sampled-data polynomial controller for nonlinear systems. *Automatica*. 2011;47(11):2457-2461.